Role of dimensionality in spontaneous magnon decay: Easy-plane ferromagnet

V. A. Stephanovich
Institute of Physics, Opole University, ulitsa Oleska 48, Opole 45-052, Poland

M. E. Zhitomirsky
Service de Physique Statistique, Magnétisme et Supraconductivité, UMR-E9001, CEA-INAC/UJF, 17 rue des Martyrs, 38054 Grenoble Cedex 9, France

(Received 23 March 2014; revised manuscript received 7 June 2014; published 23 June 2014)

We calculate the magnon lifetime in an easy-plane ferromagnet on a tetragonal lattice in a transverse magnetic field. At zero temperature magnons are unstable with respect to spontaneous decay into two other magnons. Varying the ratio of intrachain to interchain exchanges in this model, we consider the effect of dimensionality on spontaneous magnon decay. The strongest magnon damping is found in the quasi-one-dimensional case for momenta near the Brillouin zone boundary. The sign of a weak interchain coupling has little effect on the magnon decay rate. The obtained theoretical results suggest the possibility of an experimental observation of spontaneous magnon decay in a quasi-one-dimensional ferromagnet $CsNiF_3$. We also find an interesting enhancement of the magnon decay rate for a three-dimensional ferromagnet. The effect is present only for the nearest-neighbor model and is related to an effective dimensionality reduction in the two-magnon continuum.

DOI: 10.1103/PhysRevB.89.224415 PACS number(s): 75.10.Jm, 75.30.Ds, 75.50.Dd

I. INTRODUCTION

Magnons are commonly viewed as bosonic quasiparticles with integer spin $S^z = 1$. This is certainly true for isotropic ferromagnets, which were originally treated by Bloch in his seminal paper [1]. In the isotropic case the total spin (magnetization) is conserved and the magnon interaction in an isotropic ferromagnet amounts to simple particle-particle scattering or four-magnon processes [2,3]. In the presence of magnetic anisotropy, e.g., dipolar or single ion, the total spin is no longer conserved and definite spin of a magnon ceases to exist as well. As a result, additional three-particle interaction terms appear in the magnon Hamiltonian [2,4]. Spin waves in antiferromagnets have no definite value of S^z even in the isotropic case since the quantum ground state is now a superposition of states with different total spins [5]. Still, three-magnon processes appear only in noncollinear antiferromagnetic structures with completely broken spin-rotational symmetry [6,7], whereas magnon-magnon interactions in collinear antiferromagnets are represented by particle nonconserving four-magnon processes [3,8].

The special role of three-magnon dipolar processes for spin relaxation in ferromagnets was recognized already in the early works [4,9,10]. Besides that, three-particle processes may produce a spectacular quantum effect, spontaneous magnon decay, which leads to a finite magnon lifetime even at $T = 0$ [11]. Theoretical predictions of spontaneous magnon decay were made for dipolar ferromagnets [12–14], for easy-plane ferromagnets [15,16], and various noncollinear antiferromagnets (see the literature cited in Ref. [11]). At the moment there are only a few experimental evidences of spontaneous magnon decay [17–20]. Therefore, a natural question to ask theoretically is what are the physical conditions that can enhance the magnon decay rate. In the present paper we focus on the role of low dimensionality in magnon decay and specifically consider whether the decay rate is enhanced in the quasi-one-dimensional (1D) geometry. This question was previously studied in the context of quantum disordered magnets [21], but needs to be investigated for ordered magnetic systems. Our study is motivated, in part, by a prominent example of the quasi-1D easy-plane ferromagnet $CsNiF_3$ [22]. We investigate the feasibility of observing spontaneous magnon decays in inelastic neutron-scattering experiments on this material. The paper is organized as follows. In Sec. II we formulate the spin model and give the necessary details of $1/S$ spin-wave expansion. Sections III and IV are devoted to the discussion of magnon damping in the quasi-1D and the 3D cases, respectively. Section V considers the case of weak antiferromagnetic coupling between ferromagnetic chains, and Sec. VI gives our conclusions.

II. MODEL

We consider a Heisenberg ferromagnet with the easy-plane single-ion anisotropy described by the spin Hamiltonian

$$\hat{\mathcal{H}} = -J_\parallel \sum_i \mathbf{S}_i \cdot \mathbf{S}_{i+1} - J_\perp \sum_{\langle ij \rangle} \mathbf{S}_i \cdot \mathbf{S}_j + D \sum_i \left(S_i^z\right)^2 - H \sum_i S_i^z. \quad (1)$$

The nearest-neighbor exchange interactions consist of coupling $J_\parallel$ along chains parallel to the z axis and interchain coupling $J_\perp$. Without loss of generality, we consider a square-type arrangement of chains in the x-y plane (see Fig. 1). The choice $J_\parallel \simeq J_\perp$ corresponds to a 3D ferromagnet, $J_\parallel \gg J_\perp$ to a quasi-1D magnet, whereas for $J_\parallel \ll J_\perp$ a quasi-2D case is recovered. The quasi-1D ferromagnetic material $CsNiF_3$ has a significant easy-plane anisotropy with $D \approx 0.32 J_\parallel$ [22]. Motivated by this experimental example we fix in the following $D \equiv 0.3J$, where J is the largest of the two exchange constants $J = \max(J_\parallel, J_\perp)$. Since we are interested in the behavior of high-energy magnons with $\varepsilon_{\mathbf{k}} \sim J_\parallel$ we are justified to neglect the much weaker dipolar interactions in the Hamiltonian (1).

We investigate the transverse field geometry with an external field applied along the hard axis and the ferromagnetic

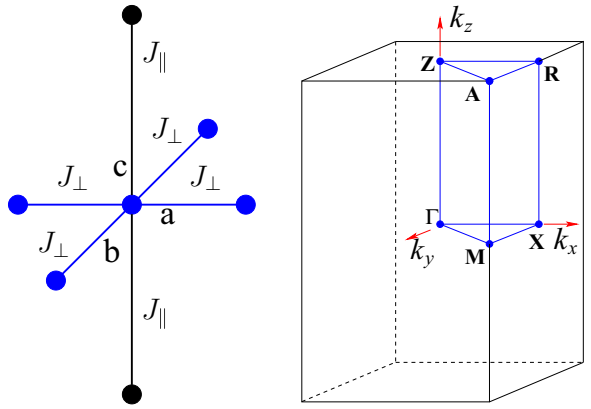

FIG. 1. (Color online) Sketch of the unit cell of a tetragonal ferromagnet with nearest-neighbor exchange interactions (left panel) and its Brillouin zone with notations for high symmetry points (right panel).

magnetization tilted from the easy plane by angle θ:

$$\sin\theta = \frac{H}{H_c}, \quad H_c = 2DS. \tag{2}$$

Above the critical field H_c the ordered moments become completely aligned with the hard axis. Note that the critical field does not depend on the ferromagnetic exchanges in (1). As a result, the strength of the three-magnon vertex remains unchanged under variations of $J_\perp/J_\parallel$ [see Eq. (5) below], and the magnon damping at fixed H solely depends on the magnon dispersion $\varepsilon_{\mathbf{k}}$ and its dimensionality.

To study excitations in the model (1) we use the transformation from spins to bosons introduced by Holstein and Primakoff [2]. As usual, the Holstein-Primakoff transformation is applied in the local frame such that the local z axis is collinear with a spin on a given site. After performing a few standard steps [11,16], including an expansion of the square roots and subsequent Fourier and Bogolyubov transformations of the magnon operators, one obtains a spin-wave Hamiltonian structured in powers of $1/S$:

$$\hat{\mathcal{H}} = \sum_{\mathbf{k}} \varepsilon_{\mathbf{k}} b^\dagger_{\mathbf{k}} b_{\mathbf{k}} + \frac{1}{2}\sum_{\mathbf{k},\mathbf{q}} V_{\mathbf{k},\mathbf{q}} [b^\dagger_{\mathbf{q}} b^\dagger_{\mathbf{k}-\mathbf{q}} b_{\mathbf{k}} + \text{H.c.}] + \cdots . \tag{3}$$

Here the magnon energy is $\varepsilon_{\mathbf{k}} = O(S)$, the three-particle (cubic) vertex responsible for spontaneous decays is $V_{\mathbf{k},\mathbf{q}} = O(S^{1/2})$, and the ellipsis stand for the higher-order terms.

An explicit expression for the harmonic magnon energy is

$$\varepsilon_{\mathbf{k}} = 2S\sqrt{A_{\mathbf{k}}(A_{\mathbf{k}} + D\cos^2\theta)}, \quad \gamma_{\mathbf{k}} = \tfrac{1}{2}(\cos k_x + \cos k_y),$$
$$A_{\mathbf{k}} = J_\parallel(1-\cos k_z) + 2J_\perp(1-\gamma_{\mathbf{k}}). \tag{4}$$

The decay vertex is given by

$$V_{\mathbf{k},\mathbf{q}} = D\sqrt{\frac{S}{2}}\sin 2\theta (g_{\mathbf{k},\mathbf{q},\mathbf{q}'} + f_{\mathbf{q},\mathbf{q}',\mathbf{k}} + f_{\mathbf{q}',\mathbf{q},\mathbf{k}}), \tag{5}$$

where $\mathbf{q}' = \mathbf{k} - \mathbf{q}$, $f_{1,2,3} = (u_1 + v_1)(u_2u_3 + v_2v_3)$, $g_{1,2,3} = (u_1 + v_1)(u_2v_3 + v_2u_3)$, and $u_{\mathbf{k}}$,$v_{\mathbf{k}}$ are the Bogolyubov coefficients:

$$u^2_{\mathbf{k}} - v^2_{\mathbf{k}} = 1, \quad 2u_{\mathbf{k}}v_{\mathbf{k}} = -DS\cos^2\theta/\varepsilon_{\mathbf{k}}.$$

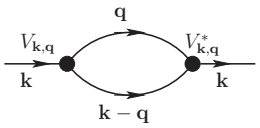

FIG. 2. The self-energy diagram corresponding to the considered two-magnon decay process.

Note that the vertex (5) has a nonmonotonous dependence on the magnetic field, $V_{\mathbf{k},\mathbf{q}} \propto H\sqrt{H_c^2 - H^2}$, resulting in the strongest amplitude for magnon decay at $H/H_c = 1/\sqrt{2}$.

For a weakly interacting magnon gas, the magnon decay rate is given by the imaginary part of the self-energy diagram shown in Fig. 2 and coincides with the Fermi's golden-rule expression:

$$\Gamma_{\mathbf{k}} = \frac{\pi}{2}\sum_{\mathbf{q}} V^2_{\mathbf{k},\mathbf{q}}\delta(\varepsilon_{\mathbf{k}} - \varepsilon_{\mathbf{q}} - \varepsilon_{\mathbf{k}-\mathbf{q}}). \tag{6}$$

The two-magnon decay processes for easy-plane ferromagnets were theoretically studied in Refs. [15,16]. Their appearance is determined by two conditions [11]: (i) the presence of the cubic vertex in the magnon Hamiltonian (3), which is a direct consequence of the fully broken spin-rotational symmetry for a state with tilted magnetization, and (ii) fulfillment of the energy conservation condition for the two-magnon decays,

$$\varepsilon_{\mathbf{k}} = \varepsilon_{\mathbf{q}} + \varepsilon_{\mathbf{k}-\mathbf{q}}, \tag{7}$$

where the harmonic magnon energy (4) can be safely used due to the smallness of the quantum effects in ferromagnets. The same kinematic conditions allow also three-magnon decays, which are present in an easy-plane ferromagnet already in zero field [16]. The amplitude of these processes is, however, rather small as they correspond to higher-order $1/S$ terms of the spin-wave expansion and we shall not consider them in the following.

Since the cubic vertex (5) depends only on D and H, the effect of dimensionality on the magnon decay rate (6) in anisotropic ferromagnets is present only via the varying dispersion $\varepsilon_{\mathbf{k}}$. The two-dimensional case was investigated in detail in our previous work [16]. In the following sections we calculate the magnon decay rate (6) for quasi-1D and 3D cases.

III. QUASI-ONE-DIMENSIONAL CASE

We begin the analysis of the magnon decay for $J_\parallel \gg J_\perp$ by treating analytically the case of long-wavelength magnons. In this limit the decay rate can be calculated perturbatively because of the smallness of the interaction among low-energy excitations and due to the reduction of the phase-space volume available for decay processes. Note that at small momenta $k,q \ll 1$, the decay vertex (5) has the standard "hydrodynamic" form $V_{\mathbf{k},\mathbf{q}} \propto \sqrt{kqq'}$. As a result, the long-wavelength excitations exhibit a usual 3D asymptote $\Gamma_{\mathbf{k}} \propto k^5$ for the decay rate [11], because the dispersion $\varepsilon_{\mathbf{k}}$ is eventually three dimensional. Therefore, the proper question to be addressed analytically is how the coefficient in the k^5 law depends on a small parameter $J_\perp/J_\parallel$.

An analytical derivation of the low-energy asymptote for $\Gamma_{\mathbf{k}}$ closely follows a similar computation for 2D or 3D magnetic systems with three-particle vertices [11]. Below we present only the essential steps. Expanding (4) in small k, one obtains

$$\varepsilon_{\mathbf{k}} \approx c\sqrt{k_z^2 + jk_\perp^2}\left[1 + \alpha k_z^2\right],$$
$$c = S\cos\theta\sqrt{2DJ_\parallel}, \quad \alpha = J_\parallel/(4D\cos^2\theta) - 1/24, \quad (8)$$

where $j = J_\perp/J_\parallel$ and $k_\perp^2 = k_x^2 + k_y^2$. Strictly speaking, the above expression for α loses its validity for $k_z \ll k_\perp$. However, as we shall see shortly, the region of interest in the quasi-1D case is $k_\perp \ll k_z$, which justifies Eq. (8).

Selecting the momentum of an incident magnon on the z axis, $\mathbf{k} = (0,0,k)$, we obtain in the same approximation

$$\varepsilon_{\mathbf{k}} - \varepsilon_{\mathbf{q}} - \varepsilon_{\mathbf{k}-\mathbf{q}} \approx -\frac{cjk}{2q_z(k-q_z)}\left(q_\perp^2 - q_0^2\right), \quad (9)$$

where $q_0^2 = 6\alpha q_z^2(k-q_z)^2/j$. Substituting (9) into the expression for the decay rate (6) and performing a separate integration of $q_\perp$ and q_z, we obtain the following long-wavelength asymptote in the quasi-1D case,

$$\Gamma_{\mathbf{k}} = a\frac{J_\parallel^2}{J_\perp}\tan^2\theta k^5, \quad (10)$$

where a dimensionless constant is $a \sim 10^{-3}$ and θ is the canting angle (2). In a 3D case for $J_\parallel = J_\perp$ a similar computation yields [15]

$$\Gamma_{\mathbf{k}} = \frac{3J_\parallel}{160\pi}\tan^2\theta k^5. \quad (11)$$

Thus, in the quasi-1D case the damping of acoustic magnons is inversely proportional to a small $J_\perp$ and is, therefore, parametrically enhanced compared to damping of acoustic magnons in 3D. We have verified such an enhancement by a direct numerical integration of Eq. (6).

Figure 3 shows the magnon decay rate (6) evaluated numerically at a representative field value $H/H_c = 0.75$ in the ΓZ direction. The curves correspond to three $J_\parallel/J_\perp$ ratios portraying crossover from a strong $J_\parallel/J_\perp = 100$ to a weak $J_\parallel/J_\perp = 10$ quasi-one-dimensionality. The two curves corresponding to $J_\parallel/J_\perp = 50,100$ exhibit large peaks in $\Gamma_{\mathbf{k}}$ near the Brillouin zone boundary, which originate from a 1D van Hove singularity in the spectrum. A more detailed structure of this peak in the inset illustrates the role of 3D coupling, which cuts off the square-root divergence of the peaks and restores 3D van Hove singularities at the boundary of the decay region and for the saddle points in the continuum. Similar 3D van Hove singularities are also prominent for small momenta towards the Γ point. Importantly, the height of the peak in $\Gamma_{\mathbf{k}}$ near the Z point decreases rapidly as the magnon dispersion becomes increasingly 3D. This demonstrates that the decays along the ΓZ direction in the Brillouin zone are most prominent for the quasi-1D case.

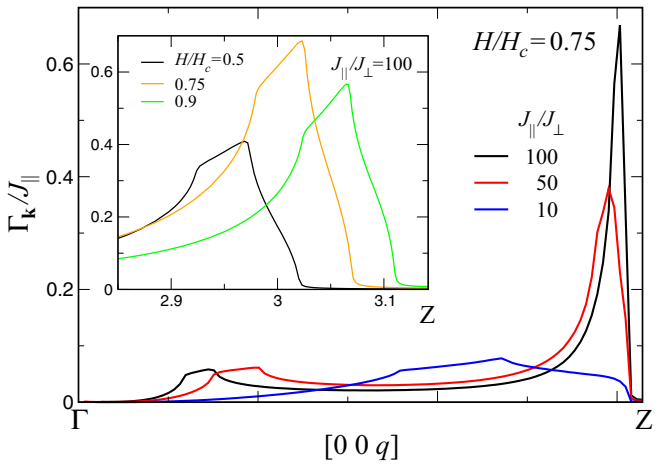

FIG. 3. (Color online) Decay rate for magnons in a quasi-1D ferromagnet for momenta along the ΓZ direction for different $J_\parallel/J_\perp$ (legend) and $H/H_c = 0.75$. The inset shows the field dependence of the peak in $\Gamma_{\mathbf{k}}$ near the Z point.

The magnetic field dependence of the magnon damping in the region, where $\Gamma_{\mathbf{k}}$ is largest, is illustrated in the inset of Fig. 3. One can see a nonmonotonous field dependence of the peak height: $\Gamma_{\mathbf{k}}$ is smallest at $H/H_c = 0.5$, it is largest at $H/H_c = 0.75$, while it again goes down at $H/H_c = 0.9$. Such a behavior is related to the field dependence of the decay vertex (5), which is zero at $H = 0$ and $H = H_c$ and has a maximum at $H/H_c = 1/\sqrt{2} \approx 0.707$.

IV. THREE-DIMENSIONAL CASE

Spontaneous magnon decays for a 2D easy-plane ferromagnet in a transverse magnetic field were studied in our previous work [16]. In particular, the decay rate $\Gamma_{\mathbf{k}}$ exhibits logarithmic peaks, which are determined by saddle-point van Hove singularities in the two-magnon density of states. Changing the type of anisotropy, exchange versus single ion, has no significant effect on the decay dynamics. Taking into account 1D (Sec. III) and 2D results [16], one can speculate that the magnon decay in 3D shows no major enhancement and thus should be small compared to low dimensional magnets.

To study the magnon damping in 3D we fix the exchange ratio to $J_\parallel/J_\perp = 1$ as an example. It is instructive to consider in this case magnons with momenta belonging to the cubic diagonal, the ΓA direction. Numerical results for $\Gamma_{\mathbf{k}}$ along this axis look very similar to Fig. 3, including a surprisingly high peak near the A point. A zoom into this region is shown in Fig. 4 for different values of an applied magnetic field. The overall shape of the numerical data is qualitatively similar to the results shown in the inset of Fig. 3 for the quasi-1D case. The peak in $\Gamma_{\mathbf{k}}$ is most prominent for $H/H_c > 0.75$, while at smaller fields it is much less pronounced. The arrows show the magnon decay boundaries, obtained from the kinematic condition $\varepsilon_{\mathbf{k}} = 2\varepsilon_{\mathbf{k}/2}$ (see further details in Ref. [11]). The above fact actually means that the predominant decay channel for a magnon in the vicinity of the damping peak is a decay into two magnons with equal momenta lying on the same cubic diagonal. With increasing H the decay region extends further towards the A point, $\mathbf{k}_0 = (\pi,\pi,\pi)$, and the two magnons emitted in a decay process become close to $\mathbf{k}_0/2$. A remarkable property of the nearest-neighbor magnon dispersion (4) near $\mathbf{k}_0/2$ is that $\varepsilon_{\mathbf{k}}$ is almost perfectly flat, with the exception of a few special directions. Such an effective dimensionality reduction is responsible for the enhanced two-magnon density of states (DOS), which in turn leads to large values of the magnon decay rate (6).

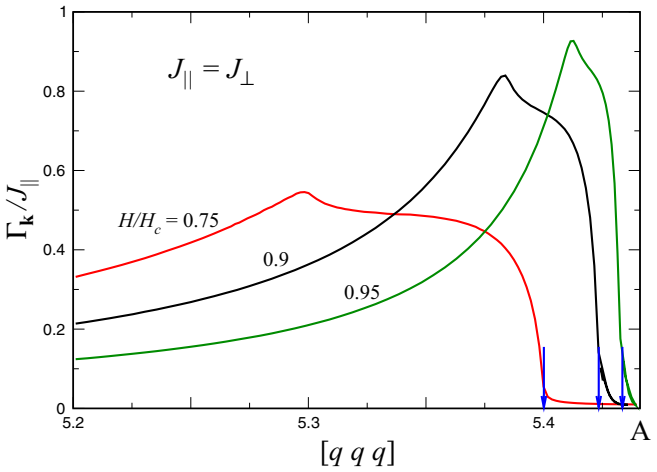

FIG. 4. (Color online) Decay rate for magnons in a 3D ferromagnet ($J_\perp/J_\parallel = 1$) with momenta along the ΓA direction for different magnetic fields (figures near curves). Vertical arrows mark the magnon decay boundaries $\mathbf{k}^*$, obtained from the kinematic condition $\varepsilon_{\mathbf{k}} = 2\varepsilon_{\mathbf{k}/2}$.

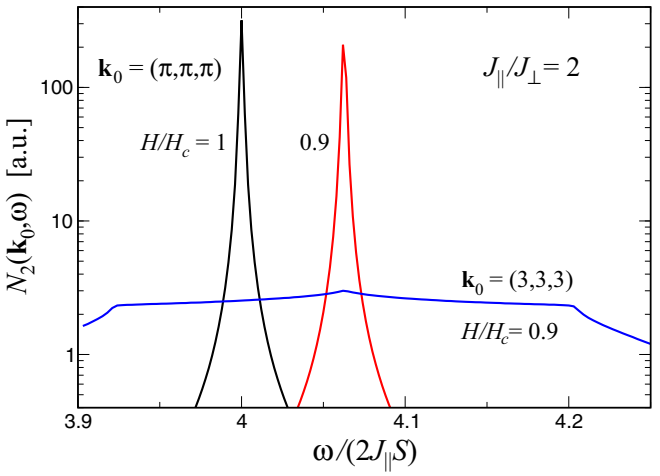

FIG. 5. (Color online) The two-magnon density of states for different values of a magnetic field (figures near curves) and $J_\parallel/J_\perp = 2$. The curve for $H/H_c = 0.9$ and $\mathbf{k}_0 = (3,3,3)$ is shown for comparison.

To check the above scenario for the magnon damping enhancement in 3D case we calculate the two-magnon DOS:

$$N_2(\mathbf{k},\omega) = \sum_{\mathbf{q}} \delta(\omega - \varepsilon_{\mathbf{k}/2+\mathbf{q}} - \varepsilon_{\mathbf{k}/2-\mathbf{q}}). \tag{12}$$

At $H = H_c$ the DOS exhibits a delta peak for $\mathbf{k} = \mathbf{k}_0$. Indeed, in that case the magnon energy (4) is given by a sum of the cosine harmonics. For $\mathbf{k} = \mathbf{k}_0$ one has $\cos(k_0/2 + q) \to \sin q$ and the sum of two magnon energies on the right-hand side of (12) yields a constant. Hence,

$$N_2(\mathbf{k}_0,\omega) = \delta\big(\omega - \varepsilon_{\mathbf{k}_0}\big), \quad \varepsilon_{\mathbf{k}_0} = 2J_0 S, \tag{13}$$

where $J_0 = 2J_\parallel + 4J_\perp$. For $H \lesssim H_c$, we expand $E(\mathbf{k}_0,\mathbf{q}) = \varepsilon_{\mathbf{k}_0/2+\mathbf{q}} - \varepsilon_{\mathbf{k}_0/2-\mathbf{q}}$ in small q as follows:

$$E(\mathbf{k}_0,\mathbf{q}) \approx 2S\sqrt{J_0 J_D}\left[1 - a_{\mathbf{q}}^2 \frac{(J_D - J_0)^2}{2J_D^2 J_0^2}\right],$$

$$J_D = J_0 + 2D\cos^2\theta, \quad a_{\mathbf{q}} = J_\parallel q_z + J_\perp(q_x + q_y). \tag{14}$$

The dependence of $E(\mathbf{k}_0,\mathbf{q})$ on $\mathbf{q}$ enters only via a linear combination $a_{\mathbf{q}}$ (14). Thus, neglecting higher-order terms, one finds an effective 1D dispersion of the decay surface $E(\mathbf{k}_0,\mathbf{q}) = \omega$. As a result, an integration of the delta function in Eq. (12) generates a conventional 1D square-root van Hove singularity in the DOS:

$$N_2(\mathbf{k}_0,\omega) \simeq \frac{1}{\cos\theta\sqrt{|\omega - 2\varepsilon_{\mathbf{k}_0/2}|}}. \tag{15}$$

At $H = H_c$ ($\theta = \pi/2$) the square-root peak transforms into the delta peak discussed above. Note also that $\varepsilon_{\mathbf{k}_0} < 2\varepsilon_{\mathbf{k}_0/2}$ for $H < H_c$ with the equality (signifying a fulfillment of the kinematic decay condition) reached only at $H = H_c$. The above analytical results for DOS can be compared with the direct numerical evaluation of (12) presented in Fig. 5.

For small departures from the $\mathbf{k}_0$ point, $H < H_c$, the two-magnon energy $E(\mathbf{k},\mathbf{q})$ acquires full dispersion on components of $\mathbf{q}$ and the van Hove singularity (15) is smeared. Still, an enhanced DOS at the former peak position survives for a range of values of $\mathbf{k}$. As an illustration, Fig. 5 shows the numerical result for $\mathbf{k} = (3,3,3)$ at $H = 0.9H_c$. A remnant peak in DOS (mind the logarithmic scale in Fig. 5) leads to a stronger decay rate $\Gamma_{\mathbf{k}}$ once the magnetic field approaches H_c and magnons with momenta close to $\mathbf{k}_0$ become unstable.

V. ANTIFERROMAGNETIC INTERCHAIN COUPLING

As was mentioned in the Introduction, our study is in a large part motivated by the quasi-1D ferromagnet $CsNiF_3$ [22]. Magnetic Ni^{2+} ions ($S = 1$) are arranged in this material in a hexagonal lattice with a ferromagnetic exchange $J_\parallel \approx 24$ K along the c axis and an antiferromagnetic interchain coupling $|J_\perp/J_\parallel| \sim 10^{-2}$. The strength of the single-ion anisotropy in $CsNiF_3$ is $D \approx 8$ K. The antiferromagnetic transition in $CsNiF_3$ takes place at $T_N = 2.5$ K, however, magnetic moments on adjacent chains do not form the 120° structure with the propagation wave vector $(1/3,1/3,0)$ expected for a triangular geometry, but rather order collinearly with $\mathbf{Q} = (1/2,0,0)$ [23]. The collinear order has been explained by a competition between the antiferromagnetic exchange and the long-range dipolar interactions [24]. In this section we consider the effect of the sign of an interchain coupling on the magnon decay in quasi-1D chains. We shall use a simplified model (1) with $J_\perp < 0$ assuming a tetragonal arrangement of chains and neglecting dipolar interactions. In this model, spin chains are still ordered ferromagnetically while an ordering between chains is described by the wave vector $\mathbf{Q} = (\pi,\pi,0)$ and corresponds to a two-sublattice antiferromagnetic structure.

We again assume that an external magnetic field is oriented along the hard axis. Theoretical calculations in this case become very similar to the spin-wave theory for a Heisenberg square-lattice antiferromagnet [7,25]. The two magnetic sublattices tilt from the easy plane by an angle θ,

$$\sin\theta = \frac{H}{2S(D + 4|J_\perp|)}. \tag{16}$$

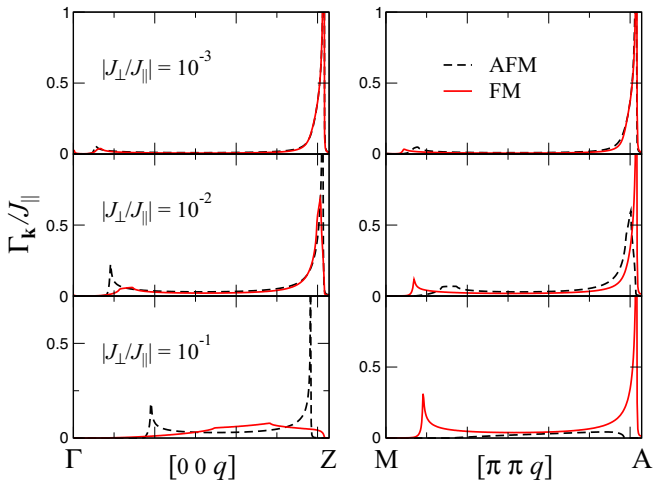

FIG. 6. (Color online) Comparison of magnon decay rates for ferromagnetic (FM, $J_\perp > 0$, solid line) and antiferromagnetic (AFM, $J_\perp < 0$, dashed line) for $H/H_c = 0.8$. Left column: ΓZ direction; right column: *MA* direction. The ratios $|J_\perp/J_\parallel|$ are 10^{-3} (upper panels), 10^{-2} (middle panels), and 10^{-1} (lower panels).

In contrast to the ferromagnetic case (2), the critical field $H_c = 2S(D + 4|J_\perp|)$ depends on an antiferromagnetic exchange $J_\perp$. After performing a standard spin-wave calculation (see Sec. II), we obtain the magnon energy

$$\varepsilon_{\mathbf{k}} = 2S\sqrt{A_{\mathbf{k}}(A_{\mathbf{k}} + D\cos^2\theta - 4|J_\perp|\gamma_{\mathbf{k}}\cos^2\theta)},$$
$$A_{\mathbf{k}} = J_\parallel(1 - \cos k_z) + 2|J_\perp|(1 + \gamma_{\mathbf{k}}). \quad (17)$$

Due to a staggered canting of spins in the antiferromagnetic structure, the three-particle term in (3) now contains $\mathbf{q}' = \mathbf{k} - \mathbf{q} + \mathbf{Q}$ instead of $\mathbf{k} - \mathbf{q}$. The explicit expression for the decay vertex is

$$V_{\mathbf{k},\mathbf{q}} = \sqrt{2S}\sin\theta\cos\theta(g_{\mathbf{k},\mathbf{q},\mathbf{q}'} + f_{\mathbf{q},\mathbf{q}',\mathbf{k}} + f_{\mathbf{q}',\mathbf{q},\mathbf{k}}), \quad (18)$$

where $f_{1,2,3} = \lambda_{1,2,3}(u_1 + v_1)(u_2u_3 + v_2v_3)$, $g_{1,2,3} = \lambda_{1,2,3}(u_1 + v_1)(u_2v_3 + v_2u_3)$, and $\lambda_{\mathbf{k}} = D - 4J_\perp\gamma_{\mathbf{k}}$.

The magnon decay rates for ferromagnetic ($J_\perp > 0$) and antiferromagnetic ($J_\perp < 0$) signs of the interchain coupling are compared in Fig. 6. The presented results illustrate a crossover from an extreme $|J_\perp/J_\parallel| = 0.001$ to a moderate $|J_\perp/J_\parallel| = 0.1$ quasi-one-dimensionality. Plots in the left column show $\Gamma_{\mathbf{k}}$ for momenta on the ΓZ line, while the right column corresponds to the *MA* cut, which includes the antiferromagnetic vector $\mathbf{Q} = (\pi,\pi,0)$ (see Fig. 1 for the notations). For a very weak interchain coupling $|J_\perp/J_\parallel| = 10^{-3}$, there is no significant difference in the magnon damping $\Gamma_{\mathbf{k}}$ between the two signs of $J_\perp$ and also between the two lines. Overall, $\Gamma_{\mathbf{k}}$ exhibits the same behavior as the results shown in Fig. 3 calculated for different values of the magnetic field. In particular, high peaks are present near the BZ boundary for both lines, ΓZ and *MA*.

Some differences start to develop for $|J_\perp/J_\parallel| \sim 0.01$ and become quite significant at $|J_\perp/J_\parallel| \sim 0.1$. The magnon dispersion between chains becomes more substantial and plays a more prominent role in the energy conservation. As a result, for the ferromagnetic interchain coupling $J_\perp > 0$, a stronger magnon damping with two characteristic peaks is present for magnons on the *MA* line, whereas $\Gamma_{\mathbf{k}}$ on the ΓZ line is significantly smaller for $J_\perp/J_\parallel = 0.1$. For the antiferromagnetic interchain coupling $J_\perp < 0$, one can observe an opposite tendency. In fact, there is a remarkable mirror symmetry between the plots on the left and on the right with a simultaneous sign change of $J_\perp$. It is related to the fact that the position of the acoustic magnon branch alters its place between the ΓZ and *MA* lines with the sign reversal. Overall, the most favorable conditions for observing spontaneous magnon decay, i.e., large $\Gamma_{\mathbf{k}}$ for an extended region in the momentum space, are found for $|J_\perp/J_\parallel| = 0.01$, a value close to the exchange ratio in $CsNiF_3$.

VI. CONCLUSIONS

In summary, magnetic excitations in an easy-plane ferromagnet placed in a transverse magnetic field become intrinsically damped at $T = 0$ due to two-magnon decays [15,16]. We have studied the effect of dimensionality on the magnon decay rate for such an ordered magnetic system. For weak interchain coupling the decay rate $\Gamma_{\mathbf{k}}$ is strongest in the vicinity of the Brillouin zone boundary exhibiting a peak $\Gamma_{\mathbf{k}} \sim 0.4$–$0.7J_\parallel$. Such a peak is related to the 1D-like van Hove singularity in the two-magnon density of states and its height needs to be compared to the characteristic energy of magnons at the Brillouin zone boundary $\varepsilon_{\mathbf{k}} = 4J_\parallel S$. For $S = 1/2$ and $S = 1$ the decay rate is a sizable fraction of the magnon energy. Therefore, spontaneous magnon decays can be observed in the neutron-scattering experiments as a significant line broadening of the zone boundary magnons. In particular, our results for a model system (1) with ferromagnetic spin chains, which are weakly coupled antiferromagnetically, indicate that spontaneous magnon decay should be prominent in the quasi-1D easy-plane ferromagnet $CsNiF_3$ [22].

Somewhat surprisingly, we have found a large decay rate $\Gamma_{\mathbf{k}}$ also in a 3D case, $J_\perp \sim J_\parallel$, for certain magnon momenta $\mathbf{k}$. The increase in $\Gamma_{\mathbf{k}}$ is again rooted in the two-magnon density of states $N_2(\mathbf{k},\omega)$ [see Eq. (12)], which develops a peak due to a very weak $\mathbf{q}$ dependence of the two-magnon energy $\varepsilon_{\mathbf{k}/2+\mathbf{q}} + \varepsilon_{\mathbf{k}/2-\mathbf{q}}$. The latter property is a consequence of the exchange coupling only between the nearest neighbors. Being a model assumption, this property is nevertheless satisfied with good accuracy in many magnetic insulators.

Overall, we conclude that lower dimensionality has a pronounced effect on spontaneous magnon decay by means of an enhanced two-magnon DOS. In the quasi-1D limit, the van Hove singularities in the DOS become largest and correspond to a strong damping of magnons in the vicinity of the decay threshold boundary. Thus, a small shift in the $\mathbf{k}$ space may lead to striking changes in the behavior of the corresponding magnon modes. Our theoretical results call for inelastic neutron-scattering measurements of the magnon lifetime in spin-chain materials. Materials with ferromagnetic chains are especially suitable for such experiments since the required magnetic fields $H \sim \max\{D, J_\perp\}$ can be rather small and the effect of magnon decay can be clearly distinguished from the spinon physics, which is present for antiferromagnetic chains.

[1] F. Bloch, Z. Phys. **61**, 206 (1930).
[2] T. Holstein and H. Primakoff, Phys. Rev. **58**, 1098 (1940).
[3] T. Oguchi, Phys. Rev. **117**, 117 (1960).
[4] A. I. Akhiezer, J. Phys. (USSR) **10**, 217 (1946).
[5] P. W. Anderson, *Basic Notions of Condensed Matter Physics* (Benjamin Cummings, Menlo Park, CA, 1984).
[6] T. Ohyama and H. Shiba, J. Phys. Soc. Jpn. **62**, 3277 (1993).
[7] M. E. Zhitomirsky and A. L. Chernyshev, Phys. Rev. Lett. **82**, 4536 (1999).
[8] A. B. Harris, D. Kumar, B. I. Halperin, and P. C. Hohenberg, Phys. Rev. B **3**, 961 (1971).
[9] E. Schlömann, Phys. Rev. **121**, 1312 (1961).
[10] M. Sparks, R. Loudon, and C. Kittel, Phys. Rev. **122**, 791 (1961).
[11] M. E. Zhitomirsky and A. L. Chernyshev, Rev. Mod. Phys. **85**, 219 (2013).
[12] V. I. Lymar and Yu. G. Rudoi, Theor. Math. Phys. **11**, 376 (1972).
[13] A. V. Syromyatnikov, Phys. Rev. B **82**, 024432 (2010).
[14] A. L. Chernyshev, Phys. Rev. B **86**, 060401(R) (2012).
[15] V. G. Baryakhtar, A. I. Zhukov, and D. A. Yablonskii, Fiz. Tverd. Tela **21**, 776 (1979) [Sov. Phys. Solid State **21**, 454 (1979)].
[16] V. A. Stephanovich and M. E. Zhitomirsky, Europhys. Lett. **95**, 17007 (2011).
[17] M. B. Stone, I. A. Zaliznyak, T. Hong, C. L. Broholm, and D. H. Reich, Nature (London) **440**, 187 (2006).
[18] T. Masuda, S. Kitaoka, S. Takamizawa, N. Metoki, K. Kaneko, K. C. Rule, K. Kiefer, H. Manaka, and H. Nojiri, Phys. Rev. B **81**, 100402(R) (2010).
[19] H. Kurebayashi, O. Dzyapko, V. E. Demidov, D. Fang, A. J. Ferguson, and S. O. Demokritov, Nat. Mater. **10**, 660 (2011).
[20] J. Oh, M. D. Le, J. Jeong, J. H. Lee, H. Woo, W.-Y. Song, T. G. Perring, W. J. L. Buyers, S.-W. Cheong, and J.-G. Park, Phys. Rev. Lett. **111**, 257202 (2013).
[21] M. E. Zhitomirsky, Phys. Rev. B **73**, 100404(R) (2006).
[22] M. Steiner, J. Villain, and C. G. Windsor, Adv. Phys. **25**, 87 (1976).
[23] M. Steiner and H. Dachs, Solid State Commun. **14**, 841 (1974).
[24] M. Baehr, M. Winkelmann, P. Vorderwisch, M. Steiner, C. Pich, and F. Schwabl, Phys. Rev. B **54**, 12932 (1996).
[25] M. Mourigal, M. E. Zhitomirsky, and A. L. Chernyshev, Phys. Rev. B **82**, 144402 (2010).